IEEE Access
Multidisciplinary | Rapid Review | Open Access Journal

Received 3 April 2023, accepted 13 April 2023, date of publication 19 April 2023, date of current version 25 April 2023.

Digital Object Identifier 10.1109/ACCESS.2023.3268544

RESEARCH ARTICLE

Probabilistic Assessment of Available Transfer Capability Incorporating Load and Wind Power Uncertainties

HALA W. REYAD, MEDHAT ELFAR, AND E. E. EL-ARABY, (Member, IEEE)
Department of Electrical Engineering, Faculty of Engineering, Port Said University, Port Said 42526, Egypt
Corresponding author: E. E. El-Araby (elsaid.elaraby@eng.psu.edu.eg)

ABSTRACT This study proposes an available transfer capability (ATC) assessment approach in an intraday market that would enable wind energy participants to raise their level of integration without exposing them to high risk. The presented methodology allows the transmission system operator (TSO) to assess ATC near to the real state while considering voltage stability concerns as well as the uncertainties of the forecasted load and wind power. The proposed formulation is designed so that the existing VAR sources are appropriately exploited during the ATC assessment to maximize its anticipated value and boost the transaction between various zones. To alleviate the complexity of analyzing N-1 contingencies in the ATC estimation, a linear sensitivity technique is applied for ranking the most severe contingencies to be examined carefully. A two-level hybrid algorithm using the primal-dual interior point method (PDIPM) and an improved grey wolf optimizer (IGWO) is suggested for solving the problem. The performance of the proposed approach has been evaluated by its application on IEEE 30- reliability test system (RTS). The outcomes confirm the viability of the proposed approach for optimizing ATC value for various transactions through the best use of installed VAR devices, considering different locations of wind farms. The obtained findings also demonstrate the effectiveness of the suggested method for determining the most severe contingency associated with each scenario under consideration.

INDEX TERMS Available transfer capability (ATC), improved grey wolf optimizer (IGWO), intraday market, reactive power dispatch, wind power generation.

I. INTRODUCTION

Recently, the integration of wind energy into electrical energy systems has increased considerably due to the economic and environmental benefits relative to conventional energy sources. However, because of the uncertainty and intermittent nature of wind energy output, large-scale wind energy integration has an obvious impact on the performance and stability of the power systems [1]. Several factors limit the increase of the penetration level of wind energy, particularly in the deregulated systems. One such substantial factor that should be precisely estimated is ATC to ensure a reliable transfer of renewable energy to remote regions. ATC is the additional transfer capability that can be transferred through a transmission line above the committed uses without violation of operational limits as defined by the North American Electric Reliability Council (NERC) [2]. To keep the power system secure and ensure smooth electric energy transactions, large-scale wind energy integration necessitates a thorough analysis of ATC evaluation. Several studies in the literature review examine ATC value, and the proposed computation approaches are primarily divided into deterministic and probabilistic methods. Related efforts employing deterministic approaches such as the continuation power flow method, optimal power flow methods, repetition power flow method, and linear approximation methods are discussed in [3], [4], [5], [6], [7], [8], [9], and [10]. Recently, because various power system factors are unpredictable, probabilistic techniques are increasingly being employed to estimate the statistical characteristics of ATC by accounting for uncertainties such as

The associate editor coordinating the review of this manuscript and approving it for publication was Ton Duc Do.

load fluctuation, generator dispatch, transmission line interruption, and renewable energy intermittency. For instance, ATC is calculated considering the system uncertainty using Monte Carlo simulation in [11] and bootstrap algorithms in [12]. In [13], the authors outline a comprehensive review of all the different probabilistic techniques which are used for ATC calculation. Prior researches [14], [15], [16], [17], [18], [19], [20], [21], [22], [23], [24], [25], [26], [27], [28], [29] have placed a greater emphasis on the influence of wind uncertainty on ATC evaluations as wind energy becomes increasingly integrated. In [14], ATC is evaluated based on an interval optimization algorithm considering the specific range of wind power uncertainty. A joint optimization approach for transmission expansion with wind power to enhance ATC is discussed in [15]. A probabilistic approach based on canonical low-rank approximation is proposed in [16] to evaluate ATC considering the uncertainties of wind power, load, and outage of transmission lines. In [17], the authors used the AC power distribution factor method to evaluate ATC, considering the reactive capability curve of the wind turbine. In [18], the author used graph theory approach to investigate the influence of incorporating capacity benefit margin in ATC assessment with considering wind energy. In [19], a bi-level optimization is proposed in which the upper level is formulated for the ATC evaluation and the lower level for economic dispatch. Optimal power flow technique is proposed in [20] to evaluate probabilistic ATC with considering wind and load side uncertainty. ATC evaluation in hybrid integrated system with considering wind uncertainty based on interval optimization technique is investigated in [21]. In [22], the authors propose an ATC probabilistic evaluation based on optimality decomposition approach and Latin Hypercube sampling technique with incorporating wind energy. ATC is calculated for online application using fast calculation technique in [23]. In [24], an average transmission congestion distribution factor method is proposed to determine the optimal location of a wind farm for ATC enhancement. ATC evaluation considering the uncertainty of wind energy based on relative distance measure arithmetic approach is presented in [25]. The solutions discussed above [14], [15], [16], [17], [18], [19], [20], [21], [22], [23], [24], and [25] allow incorporating wind power into ATC evaluation considerably easier. However, they only evaluate ATC in terms of transmission line (TL)thermal limits and voltage constraints, while overlooking the voltage stability margin that could be violated in the event of unscheduled outages, putting the system's security at risk.

Due to the complexity and computational burden, only a few research studies [26], [27], [28], [29] focused on the voltage stability issue in ATC assessment with wind energy integration. A day ahead dynamic ATC evaluation based on the Dragon Fly optimization algorithm considering high penetration of wind energy is proposed in [26]. ATC evaluation based on the risk approach with wind integration is proposed in [27]. In [28], ATC is evaluated using the interior point method while considering wind speed correlation based on Copula theory, rank correlation coefficient, and Monte Carlo simulation methods. In [29], ATC is calculated for online applications using the continuation power flow method.

Despite the above-mentioned significant Despite the above-mentioned significant contributions of the research studies [25], [26], [27], [28] which realized the necessity of taking the voltage stability issue into account in ATC assessments in the presence of wind energy, some crucial issues concerning wind power variability, contingency analysis and the effective utilization of the installed VAR devices have been overlooked and still need to be resolved. The installed VAR sources that belong to TSO have a significant effect on enhancing ATC value and ensuring voltage security. The determination of these devices' appropriate settings concurrently with the active power generation for the unexpected transition states of the system, which offers more practical solutions, has been disregarded in the preceding studies. Implementing appropriate VAR device settings as a preventive control for each individual operating period is a crucial task for the TSO in order to protect the system against any unanticipated events, such as T.L. contingency, wind power variability, and load uncertainty. Moreover, by appropriately utilizing its VAR devices, TSO can ensure precise ATC assessment and hence improve transactions across various sites. Therefore, it is essential to develop a new approach that effectively makes use of TSO' VAR devices to maintain system security and improve ATC in the presence of wind power.

This paper presents an ATC assessment methodology in an intraday market that would permit wind energy providers to improve their amount of integration with minimal risk. The current study varies from prior methods in that it seeks to properly utilize the installed VAR sources that belong to TSO for enhancing ATC value while considering the voltage stability issue as well as the uncertainties of both load demand and wind power. Since TSO possesses these devices and their control costs are inexpensive, the operator will make proper utilization of them to increase anticipated ATC. In this way, the network operator will be able to conduct, in a secure manner, more precise ATC assessment and consequently enhance transaction between different areas. Additionally, the proposed methodology gives the possibility to specify the most severe contingencies relevant for each scenario, which is vital for TSO to take into account when scheduling any transaction to endure a number of unexpected events. A two-stage architecture is proposed to achieve this goal, with the first stage determining appropriate VAR settings that improve ATC value a few hours before the real state and the second stage focusing on ATC evaluation close to the delivery time to enhance the precision of the final ATC evaluation. The proposed method incorporates the stochastic nature of load and wind power generation using a scenario-based approach, in which load and wind uncertainties are represented by normal and Weibull probability distribution functions, respectively. As the problem size gets very large due to the inclusion of voltage stability concerns and wind

power uncertainties in the proposed formulation, a linear sensitivity technique is utilized to alleviate the computational burden of ATC evaluation.

The contributions of this paper can be summarized as follows:

1- Developing a framework for evaluating ATC value close to the moment of delivery in an intraday market that would permit higher levels of wind energy integration with less risk.
2- Achieving ATC enhancement by appropriately utilizing installed VAR sources while considering voltage stability issue as well as load and wind power scenarios in the presented problem formulation.
3- Constructing a two-level hybrid algorithm using the PDIPM and an IGWO to determine the appropriate VAR dispatch that maximizes the projected ATC and subsequently improves the trade across various zones.

II. RELEVANCE OF ATC ASSESSMENT CONSIDERING LOAD AND WIND POWER UNCERTAINTIES

ATC is a crucial component in the deregulated system that the system operators must carefully assess to ensure market transparency as well as the reliability and security of the system. The precise estimation of power generated at the source area and power used at the sink area is necessary for the ATC's accurate evaluation. However, the rapid expansion of variable energy sources in several electrical markets has resulted in less predictable generation patterns. In this situation, the placement of generation on the power system with large-scale wind farms becomes uncertain, which may have a substantial impact on the accuracy of the ATC value estimated several hours ahead of the real state. These uncertainties can be reduced by more precise projections made closer to the real state of operation. Currently, several European countries have established continuous intraday markets that allow energy to be traded until shortly prior to the delivery time. For instance, in Austria, Belgium, and Germany, a quarter-hourly products are traded continuously in an intraday market. Energy can be traded up to five minutes before delivery, providing some flexibility to market participants that deal with both renewable and conventional energy [30]. The intraday markets give renewable energy providers the opportunity to minimize their risk, which makes it possible to integrate intermittent renewable energy sources more economically and in greater quantities while enhancing system security. In such circumstances, since the ATC's information forms the basis for establishing purchase and sale contracts, it is essential to precisely assess its value close to the real state to ensure efficient implementation of the market transactions. To achieve the most accurate value of ATC, it is of the essence to simulate the uncertainties of wind power outputs and loads near to the delivery time in the ATC calculation as given below.

A. ATC DEFINITION

ATC is defined by NERC as the indication of the remaining physical transmission network capability for further power transactions over already committed uses. The mathematical formulation for ATC is usually expressed as:

$$\mathrm{ATC} = \mathrm{TTC} - \mathrm{ETC} - (\mathrm{CBM} + \mathrm{TRM}) \tag{1}$$

where TTC defines the maximum transfer capability of the transmission network without violating any of a specific set of defined pre- and post-contingency constraints. ETC represents the amount of current power that can be transferred. TRM is characterized by the amount of transmission transfer capacity required to ensure that the interconnected transmission network runs securely and reliably under a reasonable range of uncertainties in system conditions. CBM is defined as the applicable margin that load-serving entities reserve to ensure access to generation from interconnected systems to meet generation reliability requirements [2]. In practice, the transfer capability margins, TRM and CBM, are typically treated as fixed values or percentages of TTC to satisfy reliability requirements. In this study, because the proposed formulation incorporates a number of factors, including load and wind uncertainties, system contingencies, as well as concerns about voltage stability, the problem will be complicated. Therefore, for the sake of clarity, the impact of these two margins will not be considered as it is in [14] and [19]. This implies that the ATC value only equals the total transfer capability less the existing power of the transmission line.

B. WIND POWER MODELING

In essence, wind speed is the main factor influencing the power output of the wind farm. However, the precise prediction of wind speed is a difficult task because it typically exhibits high variability, both geographically and temporally. According to earlier studies, the variance of wind speed at a specific location is typically described by the Weibull distribution's probability function, which accurately captures the stochastic nature of wind speed. As a result, the Weibull distribution is employed in this paper to model the variation in wind speed. This representation allows for the discretization of the PDF to provide a large number of scenarios for each study interval, which can be used to account for the unpredictable wind power output. The probability density function (PDF) of the Weibull distribution can be represented by:

$$f(v) = \frac{k}{c}\left(\frac{v}{c}\right)^{k-1}\exp\left(-\left(\frac{v}{c}\right)^{k}\right) \tag{2}$$

where v is the wind speed, k is the shape parameter and c is the scale parameter. Based on the methodology described in [31] and [32], the PDF of the wind speed is segmented into several intervals, each of which corresponds to a different scenario. The probabilities of scenarios corresponding to their estimated speeds are assessed as given in [31]. Then, the wind turbine's speed-power curve, which characterizes the relationship between wind speed and output power, is employed to calculate the wind power output from the value of wind

speed according to the following equation:

$$p(v) = \begin{cases} 0 & v \le v_{ci}, v \ge v_{co} \\ pr\dfrac{v - v_{ci}}{v_r - v_{ci}} & v_{ci} < v < v_r \\ pr & v_r \le v \le v_{co} \end{cases} \quad (3)$$

where v_{ci}, v_{co}, v_r are the cut-in, cut-out, and rated speed of the wind turbine, respectively. pr is the rated power of the wind turbine. It is important to note that the doubly fed induction generator (DFIG) is implemented as a variable speed wind generator in this study since it has the ability to control active, reactive power, and voltage, and therefore, it can be modeled as a PV or PQ bus. In this paper, the wind farm is modeled as a PQ bus with a constant power factor as a probabilistic negative load [33].

C. LOAD UNCERTAINTY MODELING

Based on historical data, the hourly forecasted load of the power system is assumed to be defined by the existing forecasting tools. The expected load errors that represent the uncertainties of the load can be described using a normal distribution with a specified mean value μ_l and standard deviation σ_l. The PDF of the generated normal distribution is then separated into specified intervals, each of which represents a certain scenario of the load. Each scenario's likelihood associated with a certain anticipated load P_l is assessed by the following equation.

$$\pi_l^d = \int_{P_l{}^{min}}^{P_l^{max}} \frac{1}{\sqrt{2\pi\sigma_l^2}} \exp(-\frac{(P_l - \mu_l)^2}{2\sigma_l^2}) dP_l \quad (4)$$

where P_l^{min} and P_l^{max} are the limits of *d-th* load scenario.

Accordingly, for a more precise ATC assessment, a scenario-based approach that combines the uncertainties of the wind power and load will be employed in the proposed approach [31]. For instance, if the normal PDF of load is split into three segments with scenario probabilities [π_l^1, π_l^2, π_l^3], and the Weibull PDF of wind speed is divided into five segments with scenario probabilities [π_w^1, π_w^{s2}, π_w^3, π_w^4, π_w^5], then there are a total of 15 scenarios under consideration, and their pertinent probabilities are as follows:

$$[\pi_w^1\pi_l^1, \pi_w^1\pi_l^2, \pi_w^1\pi_w^3, \ldots\ldots\ldots\ldots, \pi_w^5\pi_l^1, \pi_w^5\pi_l^2, \pi_w^5\pi_l^3]$$

It should be noted that a key issue with our formulation is that the problem's size and complexity have grown greatly in comparison to earlier formulations. This is because significant factors such as load and wind uncertainty, N-1 contingencies, and concerns about voltage stability have been considered. Therefore, for the sake of simplicity, we assume that the variability of the wind speed and load is constant, and the specified mean and standard deviation relevant to the wind speed and load demand are employed to represent merely their uncertainties, as given above.

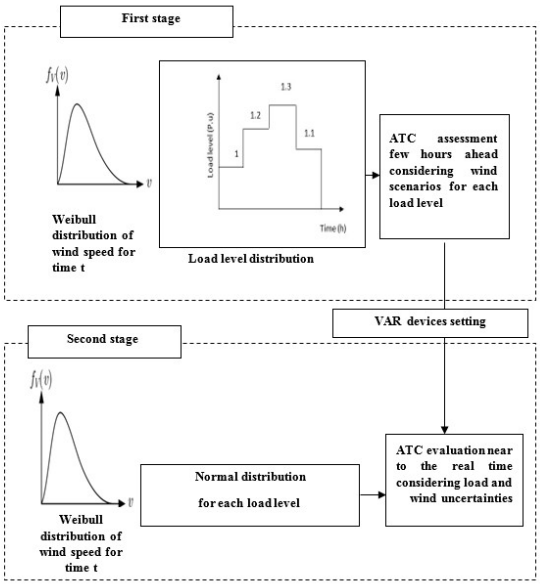

FIGURE 1. Proposed method.

III. PROPOSED METHOD

This section focuses on the suggested ATC assessment and improvement method that takes into account the integration of the wind power and load scenarios described in the previous section. The proposed approach is split into two layers that can be summarized in Fig. 1. At the first level, we assume that the wind power producers are integrated as a part of a continuous intraday market and that the system operator is supposed to evaluate ATC a lead time before the delivery time. Depending on the rules of the market, this lead time could be from an hour to a few hours prior to the actual state. At this level, since the system operators are eager to precisely assess and maximize the power transfer between different areas, all of the system's available existing controllers are employed to achieve this purpose. Since the VAR dispatch is one of the primary techniques contributing to the enhancement of the ATC and system security, it has been employed to determine the adequate settings of the VAR devices at the first level. The VAR settings will be established and regarded as fixed for a certain period specified by the system operators. For instance, if the ATC is being evaluated four hours ahead of the delivery time, the load will be forecasted and treated as fixed for a specific interval that will be decided by the system operator over the course of the following four hours. This interval could be an hour, a half hour, or a quarter-hour depending on how closely the first stage has been completed and the required accuracy set by the system operator. The optimal VAR dispatch will be carried out at each particular interval, considering the previous wind power scenarios with the goal of maximizing ATC. It is worth mentioning that the first stage is solved using a hybrid approach that incorporates IGWO and the conventional PDIPM as will be shown in section V. Using the VAR dispatch obtained in this stage, ATC will be assessed very close to the delivery time "an

hour to 15 minutes before real-time'' in the second level. In the second stage, an integration of load and wind scenarios at each time interval is employed for ATC evaluation. It should be emphasized that even though at this stage only the forecasted load can be employed and simulated at each interval, integrating load and wind power scenarios greatly enhances the precision of the final ATC assessment. The problem at the second level is formulated as a large-scale nonlinear programming problem with the goal of maximizing probabilistic ATC, and it has been solved using the interior point approach, as will be described in section V.

IV. PROBLEM FORMULATION

In the following subsections, the detailed problem formulation for the first and second stages is provided.

A. FIRST-LEVEL FORMULATION

At this stage, the system's available existing controllers that represent the decision variables are utilized to maximize ATC for a set of wind power scenarios and different load levels. The decision variables include the generator active power of the conventional source as well as VAR control devices, including SVCs, the generators' reactive power, LTC transformer taps, and shunt capacitors. For each load level, the problem is stated as an optimization problem given by Eq. (5) to Eq. (7), where its objective function is the maximization of the anticipated ATC, which is represented by the expected load margin associated with the wind power scenarios as given by Eq. (5). The objective function is achieved while satisfying several operational constraints representing extended power flow Eq. (6), and operational limits of the state and control variables as defined by Eq. (7). The objective function and operational constraints can be expressed as follows:

$$\text{Maximize ATC} = \min(-(\sum_{s=1}^{ns} \pi_w^s \lambda^s)) \tag{5}$$

$$\text{Subject to } y_0^s + \lambda^s y_d^s - g\left(x^s, u_g^s, u_v^s\right) = 0, \quad s = 1, 2, \ldots ns \tag{6}$$

$$h_{min} \le h\left(x^s, u_g^s, u_v^s\right) \le h_{max}, \quad s = 1, 2, \ldots ns \tag{7}$$

where superscript s = (1,2…, *ns*) indicates the wind power scenario, λ is the scalar parameter representing load power margin, π_w^s represents the probability of *s-th* wind power scenario, *ns* is the number of wind power scenarios, y_0 is the mismatch vector, y_d is the load direction vector, *g* stands for the power flow equations, *x* is the state variables vector including voltage magnitudes of load buses and loading of the transmission line P_{ij} from bus *i* to bus *j*, u_g is the generator control variables vector comprising real and reactive power of generator buses, u_v is the VAR control devices vector consisting of shunt capacitors, transformer tap changer, SVCs, and extra.

Note that the effect of wind power generation (active and reactive power) is taken into consideration in the load flow constraints as in Eq. (6), by integrating their values into the mismatch vector y_0. Furthermore, we assume that VAR devices u_v that are already present in the systems will be dispatched and considered fixed in the second stage. Since these devices belong to TSO and their control costs are very cheap, they will be appropriately utilized by TSO to maximize the expected ATC.

1) RANKING BRANCH OUTAGE CONTINGENCIES

An ATC estimate requires analyzing the uncertainties regarding the system contingencies, which include the probabilistic outages of generators and transmission lines. In this study, line outage will be merely considered in the ATC evaluation, as in several previous studies. Furthermore, for a more conservative decision for TSO, the probability of a line outage is assumed to be 100% in this paper, as it was in most earlier studies on ATC evaluation. As the ATC estimation needs to analyze N-1 contingencies, it will be a computational burden, especially for large power system simulation. The inclusion of wind power scenarios in the proposed formulation significantly increases the size of the problem, and hence the amount of required computational effort. Therefore, ranking contingencies to quickly identify the ones that have the most serious impact on the electrical power system's voltage stability and ATC value is a crucial issue to make computing time reasonable. In this paper, the sensitivity-based approach introduced in [34] and [35] that evaluates rapidly the load power margins for outage contingencies is carried out to alleviate the computational time concern. The post-fault load power margin value is used for ranking the most severe contingencies since it is widely accepted as the most informative index, directly representing the degree of voltage stability problem. In order to evaluate the post-fault load power margin for a specific contingency, two main steps should be executed. First, pre-contingency load power margin, bus voltages, and left/right eigenvectors corresponding to the minimum eigenvalue at the nose point should be determined. The point of collapse method or singular value decomposition (SVD) technique can be used to calculate these values for each wind scenario. This calculation is performed just once and is regarded as a prime computation. This implies that the obtained values at the pre-contingency will commonly be used as fixed values for all of the post-contingencies associated with each scenario. To achieve that, the set of equations characterizing the conditions for the saddle-node bifurcation in the post-contingency case are linearized around the pre-fault bifurcation point. The conditions of saddle-node bifurcation for each wind scenario are given as follows:

$$f\left(x^c, u_g^c, u_v^c, p\right) = y_o + (\lambda^c) y_d - g\left(x^c, u_g^c, u_v^c, p\right) = 0 \tag{8}$$

$$w^T g_x\left(x^c, u_g^c, u_v^c, p\right) = 0, \quad ||\mathrm{w}|| \neq 0 \tag{9}$$

or

$$g_x\left(x^c, u_g^c, u_v^c, p\right) \eta = 0, \quad ||\eta|| \neq 0 \tag{10}$$

where superscript c indicates the collapse point, g_x is the power flow Jacobian matrix, w is the left eigenvector, η is the right eigenvector. To characterize branch outages, each branch admittance is expressed using the contingency parameter p as follows:

$$(1 - p^k)y_{ij}$$

where y_{ij} depicts the admittance of line to be faulted, $p^k = 0$ denotes the pre-fault situation and $p^k = 1$ refers to postfault for contingency k.

In accordance with the proposal published in [34] the aforementioned Eq. (8) to Eq. (10) are linearized around the pre-fault bifurcation point. The linearized equations are then rearranged to provide the following equation (11) to predict the change in load margin $\Delta\lambda$ for the post-fault contingency.

$$\Delta\lambda = \frac{-w^T f_p}{w^T f_y} \tag{11}$$

Then, the post-fault $\bar{\lambda}$ may be easily determined using the pre contingency $\underline{\lambda}$ found by Eq. (5) to Eq. (7) as follows:

$$\bar{\lambda} = \underline{\lambda} + \Delta\lambda \tag{12}$$

One can get more information about Eq. (8) to Eq. (10), and the derivation of Eq. (11) in [34] and [35].

2) FIRST-LEVEL SOLUTION STEPS

Based on the above equations, the calculation steps for ATC evaluation using PDIPM can be summarized as follows:

1- Read system data and define transfer patterns ''point to point'' and ''area to area'' for ATC evaluation.
2- Maximize pre-contingency load margin $\underline{\lambda}$ by using Eq. (5) to Eq. (7) and specifying its value for each scenario.
3- For each wind scenario, define the pre-contingency $\underline{x}$, $\underline{w}$ *and* $\underline{\eta}$ using the SVD method.
4- For each scenario, estimate $\bar{\lambda}$ for all contingencies using Eqs. (11) and (12), then choose the most severe contingency related to each scenario that is the smallest one.
5- Evaluate the expected ATC using Eq. (5) to Eq. (7), for the most severe contingencies.

It is worth mentioning that the above procedures will be carried out while the VAR control devices μ_v are fixed for the pre- and post-contingency instances. This implies that the preventive control mode is assumed by setting $\Delta\mu_v = 0$. This presumption guarantees that the VAR dispatch will be executed without adjustment for the base case and contingency circumstances for a given period while considering wind power scenarios.

B. SECOND-LEVEL FORMULATION

As discussed before, the second stage is interested in the ATC evaluation very close to the delivery time in order to enhance the precision of the final ATC value. The two key distinctions between the second level and the first level are the incorporation of the load scenarios into problem formulation and the treatment of u_v^s, which is regarded as fixed in this situation. Hence, at this stage, the decision variables are identical to those at the first level, except for u_v, while the state variables vector is the same as the first level. The proposed problem formulation, which deems u_v^s is fixed while integrating the load and wind scenarios, can be stated as follows:

$$\text{ATC} = \min(-(\sum_{s1=1}^{n_c} \pi_c^{s1}\lambda^{s1})) \tag{13}$$

$$\text{Subject to } G^{L2}\left(x^{s1}, u_g^{s1}, \mu_v, \lambda^{s1}\right) = 0,$$
$$s1 = 1, 2, \ldots\ldots n_c \tag{14}$$
$$H^{L2}\left(x^{s1}, u_g^{s1}, \mu_v\right) \le 0,$$
$$s1 = 1, 2, \ldots\ldots n_c$$
$$\pi_c^{s1} = \pi_w^s \pi_l^d, \quad n_c = n_s n_d \tag{15}$$

where G^{L2} and H^{L2} are identical to the constraints as in Eqs. (6) and (7), respectively, except that the superscript $L2$ denotes the second stage. π_l^d is the probability of the *d-th* load scenario. n_d is the number of load scenarios.

It is important to note that, although the load scenarios are included in the calculation above, it is still possible to simulate the forecasted load ''without its related scenarios'' for the specified time if the load is anticipated perfectly. The decision of whether to take the load forecasting errors into consideration or not depends on the accuracy that the system operator requires.

V. PROPOSED SOLUTION ALGORITHM

The problem formulations of the first and second levels introduced in the previous section are stated as large-scale nonlinear optimization problems. In the first level, while wind power scenarios are taken into consideration, the load for the designated period is treated as constant. The purpose is then to achieve the proper dispatch of VAR devices that maximize expected ATC for the particular time period selected by the system operator. These VAR devices will be the same for each simulated wind power scenario. The problem in this instance cannot be handled by using standard nonlinear optimization techniques alone due to the complexity and the scale of the problem formulation. Therefore, a hybrid algorithm using IGWO and PDIPM is used to solve the first-level problem as in Eq. (5) to Eq. (7). At the second level, the VAR dispatch that was obtained at the first level is then regarded as fixed. With this treatment, the second level's problem size is drastically reduced, making it much simpler to solve than the first level. Consequently, PDIPM has been employed straightforwardly at the second level to obtain the best ATC assessment close to the real state. Fig. 2 provides a summary of the computational procedures of the proposed approach for solving the first-level problem. The proposed solution, as depicted in the figure, starts with random initial candidates ''*m*'', with each candidate in the population standing for a potential VAR dispatch solution. Each candidate pattern is used commonly for each wind power scenario associated with the base case and all contingency states under investigation. In the base case, the optimization problem as in Eq. (5) to

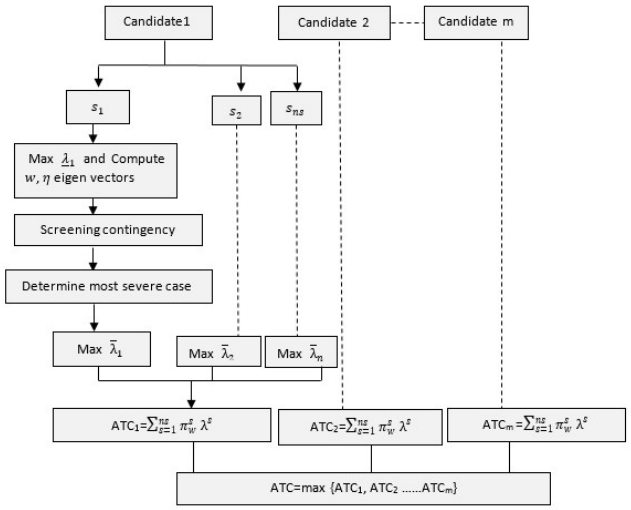

FIGURE 2. A hybrid GWO/PDIPM solution method (Fist level problem).

Eq. (7) is solved using PDIPM for each scenario separately to determine $\underline{\lambda}$. Meanwhile, SVD method is performed to determine, $\underline{x}$, $\underline{w}$ *and* $\underline{\eta}$ to be used for the contingency screening where Eqs. (11) and (12), are utilized to quickly ascertain the approximate value of $\bar{\lambda}$ for each contingency. Accordingly, the most severe contingency associated with each wind power scenario is defined. The optimization problem as in Eq. (5) to Eq. (7) is then solved for the most severe contingencies separately using PDIPM to identify the precise value of $\bar{\lambda}$ associated with each wind power scenario. Then, the expected ATC related to each candidate can be calculated using the probability of the wind power scenario and the value of $\bar{\lambda}$ related to each scenario. These procedures are performed for each candidate in the population. Among the candidates, the actual expected ATC for the current iteration is picked as the maximum expected ATC. The IGWO operators are then utilized to update the next population where each individual is a new candidate for VAR devices. This procedure is repeated till the termination criterion is satisfied.

In this work, IGWO is used because it is indicated in [36] that it achieves the balance between exploitation and exploration in the search space and has a faster convergence rate than other heuristic algorithms for reaching the global optimal solution. The following subsection shows an overview of GWO and its computational procedures for solving the proposed formulation.

A. GWO OVERVIEW

The GWO is a metaheuristic technique that was first presented in [36] and [37]. It is based on the natural hunting strategy of grey wolves, who have a social hierarchy system with four groups designated α, β, δ, and ω. The algorithm considers wolves α, β, and δ as the best candidates to guide the ω wolves toward the searching area in order to find the overall solution. The three basic components of the hunting mechanism are searching for the prey, encircling the prey, and attacking it can be mathematically described as given below.

1) ENCIRCLING PREY

During the hunt, grey wolves encircle their prey. Below is a mathematical representation of the encircling behavior:

$$D = |C.G_P(N) - G(N)| \tag{16}$$

$$G(N+1) = G_P(N) - A \cdot D \tag{17}$$

where G_P stands for the position of the prey, G is a grey wolf's position vector, and N is the current iteration. The coefficient vectors C and A are as follows:

$$A = 2\vec{a} \cdot \text{rand1} - \vec{a} \tag{18}$$

$$C = 2 \cdot \text{rand2} \tag{19}$$

where the components of the vector $\vec{a}$ are linearly lowered from 2 to 0 throughout the iterations, rand1 and rand2 are random vectors in the range [0, 1].

2) HUNTING

The mathematical modeling of the hunting behavior assumes that α, β and δ wolves have better knowledge about the location of the prey, Therefore, the other wolves ω update their positions in accordance with α, β and δ wolves' positions as they consider them to be the three best solutions as follows:

$$\begin{aligned} D_\alpha &= |C_1 \cdot G_\alpha - G(N)|, \\ D_\beta &= |C_2 \cdot G_\beta - G(N)|, D_\delta = |C_3 \cdot G_\delta - G(N)| \end{aligned} \tag{20}$$

$$G1(N) = G_\alpha - A_1 \cdot D_\alpha, \quad G2(N) = G_\beta - A_2 \cdot D_\beta,$$

$$G3(N) = G_\delta - A_3 \cdot D_\delta \tag{21}$$

$$G(N+1) = (G1(N) + G2(N) + G3(N))/3 \tag{22}$$

where C_1, C_2, and C_3 are computed by (19). G_α, G_β, and G_δ are the first three best positions at iteration N. A_1, A_2, and A_3 are calculated as in Eq. (18), and D_α, D_β, and D_δ are given by Eq. (20).

3) ATTACKING

When the prey stops moving, the hunting process is ended, and the wolves launch an attack. Mathematically, this is represented by the value of $\vec{a}$, which progressively decreases from 2 to 0 over the duration of iterations, controlling the exploration and exploitation.

B. IMPROVED GWO

The position of each wolf is updated in the conventional GWO with the aid of the three best grey wolves as a mean value of them. This results in slow convergence and a limitation of population diversity, and the wolves may as a result get trapped in local optima. In order to improve the search strategy of wolves while hunting, the presented method in [36] is employed to overcome these deficiencies. This strategy is called dimension learning-based hunting (DLH). In DLH, each individual wolf is learned by its various neighbors that it can be a potential candidate for the new position of $Gm(N)$.

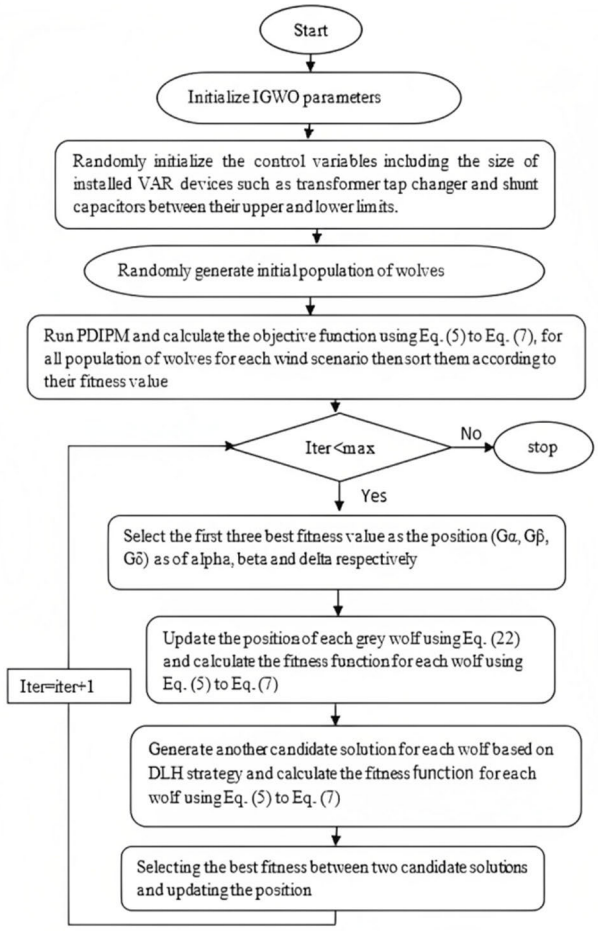

FIGURE 3. Solution procedures for the first stage.

As a result, IGWO has both candidate wolves produced by the GWO and the DLH search hunting methods for each iteration in order to get a superior position. The IGWO algorithm then evaluates the two candidates to identify the best candidate wolf for updating the current position in the following iteration. The details of the IGWO are given in [36]. In this paper, the IGWO is implemented with PDIPM for solving the first-level problem. The computational steps combining IGWO and PDIPM for solving the first level problem in Eq. (5) to Eq. (7) are simplified by the flow chart shown in Fig.3.

Note that, in the second level, the final expected ATC close to the real state is evaluated using the VAR dispatch acquired at the first level in accordance with the algorithm presented in Fig. 3, where the PDIPM technique is merely applied as a solution methodology for the problem in Eq. (13) to Eq. (15).

VI. SIMULATION RESULTS AND DISCUSSION

The proposed method has been implemented on IEEE 30-bus RTS, which is divided into three areas as shown in Fig. 4. The simulations were conducted in the MATLAB platform using a PC with an Intel Core i7-7500U CPU, 2.7 GHz, and 8 GB RAM. The original system has been modified to incorporate a 100 MW wind farm, which is an aggregate of several turbines.

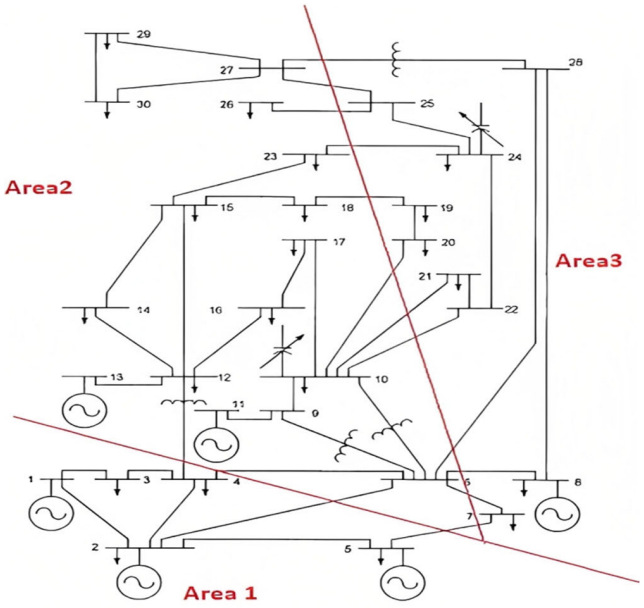

FIGURE 4. Single line diagram of IEEE-30RTS.

The technical parameters of the employed wind turbines are provided in [31]. The impact of the 100 MW wind farm on ATC value will be analyzed when it is independently installed at bus 2 ''generation area'' or bus 28 ''sink area'', respectively. The bus voltage magnitudes are specified to be within the range of 0.9–1.1 p.u., while the installed VAR devices ''capacitor banks and SVCs'' are supposed to vary between 0 and 0.4 p.u., and the limits of on-load tap changers are between 0.9 and 1.1 p.u. Since the ATC is assessed at two levels in the proposed formulation, it is important to first identify the initial requirements explicitly for each stage. At the first stage, ATC is supposed to be estimated 4 hours ahead, where their associated load levels are 100%,120%, 130%, and 110% of the original system load. Since the ATC is being evaluated preliminary at this stage, it is unessential to examine numerous scenarios for the sake of reducing the computational burden. Therefore, in the first stage, we have examined only the five wind power scenarios given in Table 1 for each load level. The proposed hybrid IGWO/PDIPM solution technique is used to solve this stage, where the population size of wolves is assumed to be 25, and the maximum number of iterations is set to 50. The results of the VAR dispatch obtained at the first level will be settled in the second stage to evaluate ATC close to real time. In the second stage, as the ATC assessment is the final expected value that affects the ultimate decision of market participants, a more precise estimation is conducted by including the combination of the load scenarios and more scenarios from wind power. The wind power and load scenarios with their associated probabilities employed in the second stage are given in Table 2 and Table 3, respectively. The ATC values at the first and second stages are determined by simulating single-bilateral transaction T1 and multilateral transaction T2, given in Table 4. The following

TABLE 1. Wind power scenarios of the first stage.

Scenario number	Prob of each scenario	Active power output (p.u)
S_1	0.0689	0
S_2	0.2044	0.1287
S_3	0.4048	0.4937
S_4	0.1992	0.8683
S_5	0.1227	1

TABLE 2. Wind power scenarios of the second stage.

Scenario number	Prob of each scenario	Active power output (p.u)
S_1	0.0680	0
S_2	0.0565	0.05
S_3	0.0734	0.15
S_4	0.0872	0.25
S_5	0.0966	0.35
S_6	0.1006	0.45
S_7	0.0989	0.55
S_8	0.0921	0.65
S_9	0.0814	0.75
S_{10}	0.0684	0.85
S_{11}	0.0545	0.95
S_{12}	0.1223	1

three cases are thoroughly examined for simulating T1 and T2 to assess the developed method.

A. CASE I: WIND FARM AT THE GENERATION CENTER

In this case, the location of the wind farm is assumed to be at bus 2. ATC is evaluated for bilateral transaction T1 and multilateral transaction T2. For each load level listed in Table 3, the five wind power scenarios and their associated probabilities given in Table 1 are employed in this stage. Table 5, which displays the settings of VAR devices and

TABLE 3. Load scenarios of the second stage.

Scenario number	Load percentage %	Load probability
1	96.9482	0.1587
2	100	0.6826
3	103.0518	0.1587

TABLE 4. Transaction classification.

Transaction	Seller		Buyer	
	Area	Bus no	Area	Bus no
T1	1	1	3	24
T2	1	1,2	2,3	23,24

provides the maximum predicted ATC value for each load level, gives the results for this stage. It should be noted that the values in the table for Qc10 and Qc24 correspond to shunt capacitors installed at buses 10 and 24, respectively. Additionally, T(6-9), T(6-10), T(4-12), and T(28-27) refer to the on-load tap changer settings for the respective lines (6-10), (6-9), (4-12), and (27-28). The results show that the ATC value for any transaction decreases with increasing load levels for each transaction. Fig. 5 depicts the convergence curve for T2 at 100% of the system's typical load. According to the convergence characteristic, the objective function converges smoothly after 25 iterations. The execution time for this stage is 2639 seconds.

In the second stage, ATC is evaluated very close to the delivery time. In order to improve the accuracy of the final ATC assessment, the wind power scenarios shown in Table 2 are combined with the load scenarios of each load level shown in Table 3. Therefore, this stage is solved for 36 scenarios acquired by combining the 12 wind power scenarios depicted in Table 2 with the 3 load scenarios given in Table 3, where their overall associated probabilities are obtained by multiplying the respective probabilities of the wind power and load. For each of the 36 examined scenarios, the obtained VAR settings from the first stage have been considered constant values. Table 6 lists the results for this stage, which shows the expected ATC value for the base case and post-contingency case for each load level. As shown in the table, the post-contingency case values are lower than the base case values, and the ATC value drops as transaction load levels rise. The ATC values are lower when compared to the first stage's results, which are displayed in Table 5. This is because in this situation, more scenarios are investigated, and one of the examined load levels is higher than the predicted load by

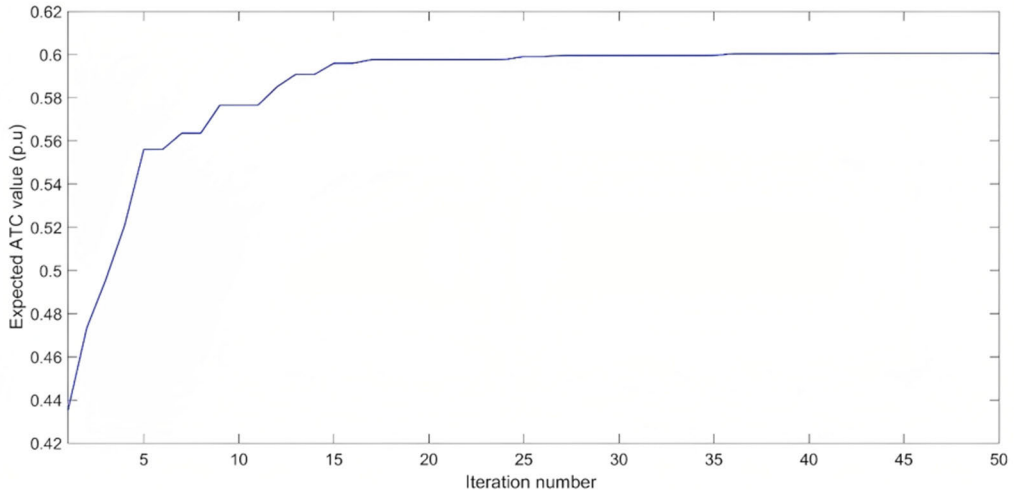

FIGURE 5. Convergence characteristic of the proposed method for T2.

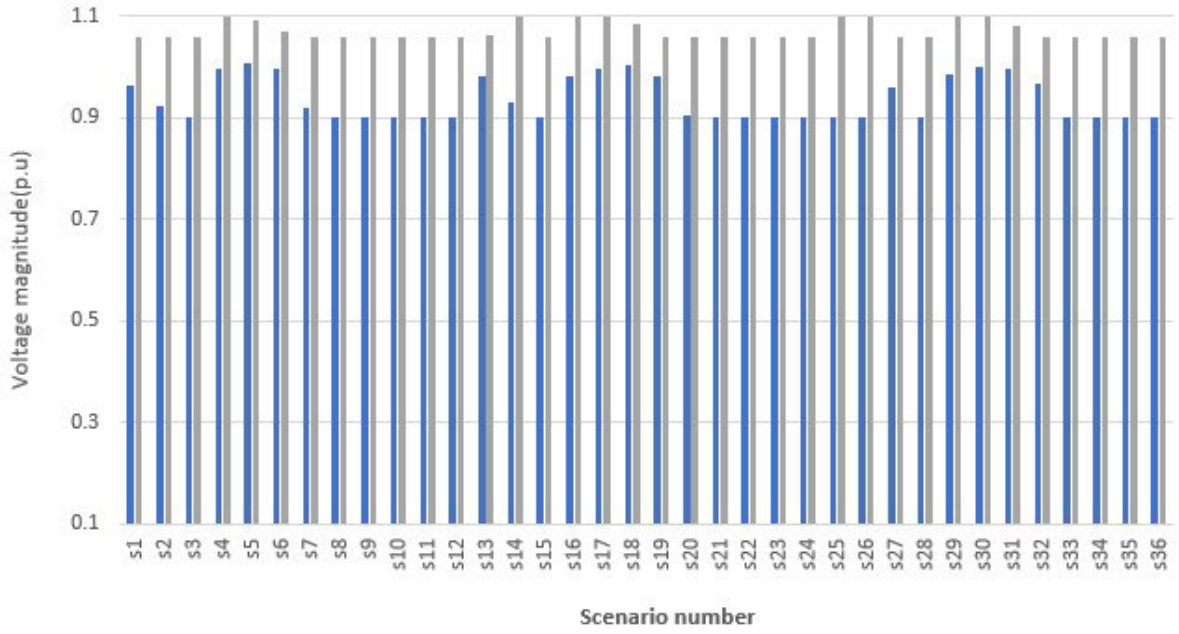

FIGURE 6. Maximum and minimum voltage magnitudes for all scenarios for T2.

about 3.1%, leading to a more conservative decision. Also, the table lists the most severe contingency case related to each scenario, which is important for the system operator to take into account for any line outages that might occur for any transaction. For example, the most severe lines for 100% of the original system load for T1 are lines (1-3), (2-6), and (22-24). This implies that the evaluated ATC value in the proposed method addresses not only one severe contingency, but numerous serious ones correlated with the invigilated scenarios, making it more conservative for a variety of potentially uncertain circumstances. Fig. 6 shows the minimum and maximum voltages for each scenario for the load level of 130% of the normal load for T2. The figure shows that the transaction can be obtained using the proposed method while maintaining the voltage for all scenarios between the minimum and maximum voltage limits. The execution time for this stage is 112 seconds.

B. CASE II: WIND FARM AT THE LOAD CENTER

In this case, the wind farm is presumed to be situated near the load center at bus 28, and ATC is then assessed for bilateral transaction T1 and multilateral transaction T2. Table 7 illustrates the final solution of the first stage, displaying the maximum expected ATC value for the post contingency for each load level as well as the settings of the VAR sources. The results, which are shown in the table, indicate that the ATC value for any transaction decreases as the load level is increased.

TABLE 5. Settings of VAR devices and expected ATC value for the first stage.

Transaction	Load level(p.u)	Settings of VAR sources(p.u)						Expected ATC value for Post-contingency case (p.u)
		Qc_{10}	Qc_{24}	T(6-9)	T(6-10)	T(4-12)	T(28-27)	
T1	1	0.088	0.056	1.008	1.088	0.965	1.073	0.686
	1.2	0.002	0.399	0.926	0.901	1.089	1.031	0.373
	1.3	0.242	0.220	0.961	0.998	0.977	1.026	0.308
	1.1	0.330	0.049	0.933	1.095	1.081	0.910	0.473
T2	1	0.387	0.083	0.948	0.935	0.939	1.091	0.601
	1.2	0.398	0.233	0.904	1.092	1.098	1.049	0.358
	1.3	0.285	0.324	0.995	1.066	1.014	0.961	0.209
	1.1	0.254	0.359	1.091	1.069	1.046	0.960	0.506

TABLE 6. Expected ATC value for the second stage.

Transaction	Load level(p.u)	Expected ATC value (p.u)		Most severe contingency for each scenario
		Base _case	Post-contingency case	
T1	1	0.777	0.642	Line1-3 (for s1, s2, s3, s13, s14, s25, s26, s27, s 29)
				Line2-6 (For s15, s28)
				Line22-24 (for the other scenarios)
	1.2	0.469	0.313	Line2-6 (for s6, s19, s31, s32)
				Line1-3 (for the other scenarios)
	1.3	0.356	0.245	Line1-2 (for s1, s2 ,s13, s15)
				Line 2-6 (for s5, s17, s18, s30, s31)
				Line1-3 (for the other scenarios)
	1.1	0.596	0.415	Line2-6 (for s3, s15, s28)
				Line1-3 (for the other scenarios)
T2	1	0.652	0.600	Line1-3 (for s 1, s 2, s3 , s4, s13, s14, s15, s16, s25 , s26, s27, s28, s29, s30)
				Line9-11 (for the other scenarios)
	1.2	0.405	0.297	Line2-6 (for s1, s2, s13, s 14, s27)
				Line1-3 (for the other scenarios)
	1.3	0.272	0.148	Line1-2 (for s3)
				Line2-6 (for s1, s2 ,s13, s15, s27, s28)
				Line1-3 (for the other scenarios)
	1.1	0.594	0.506	Line2-6 (for s1, s13, s14)
				Line1-3 (for the other scenarios)

It is clear that the value of ATC at any transaction for the same load level is slightly higher compared to the outcomes of the first stage of Case I. For instance, the ATC in Case II for transaction T2 at load level 1.1 is 0.615 while it is 0.506 in Case I. This is due to the wind farm's proximity to the load center in Case II, which lowers transmission losses and hence improves transfer capacity. The convergence characteristic for T1 at a load level equal to 130% of the original system load is shown in Fig. 7. The execution time for this stage is 2276 seconds.

In the second stage, load uncertainty is considered instead of the forecasted load for each interval, and simulation has been performed using the same 36 scenarios that were used in Case I. With the help of the VAR settings decided at the first stage, which are shown in Table 7, Table 8 presents the outcomes of the expected ATC values for the base case and

TABLE 7. Settings of VAR devices and expected ATC value for the first stage (Case II).

Transaction	Load level	settings of VAR resources(p.u)						Expected ATC value for post-contingency case (p.u)
		Qc_{10}	Qc_{24}	T (6-9)	T (6-10)	T (4-12)	T (28-27)	
T1	1	0.085	0.216	0.989	0.949	0.941	0.919	0.736
	1.2	0.103	0.088	0.995	1.009	1.009	1.061	0.514
	1.3	0.231	0.118	1.059	1.039	0.996	1.033	0.362
	1.1	0.139	0.002	0.979	1.064	0.938	1.094	0.561
T2	1	0.157	0.361	1.021	1.093	0.916	0.917	0.656
	1.2	0.313	0.031	1.003	0.916	0.904	1.075	0.429
	1.3	0.291	0.174	0.919	0.906	1.075	1.068	0.339
	1.1	0.060	0.229	0.928	1.076	1.068	0.989	0.615

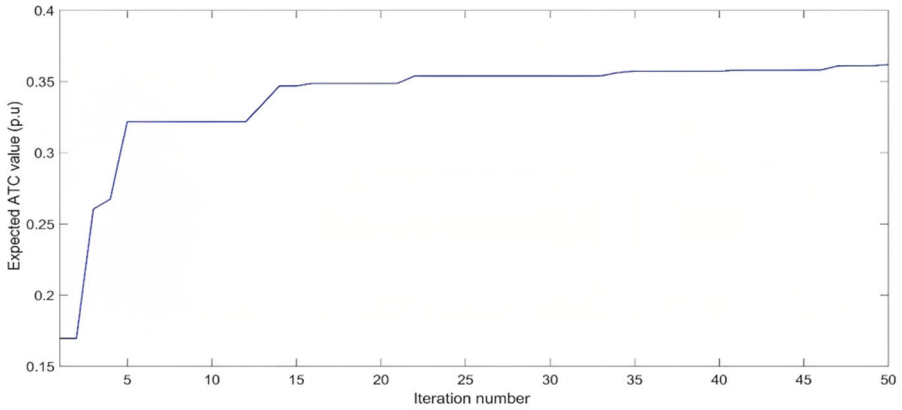

FIGURE 7. Convergence characteristic of the proposed method for T1 (Case II).

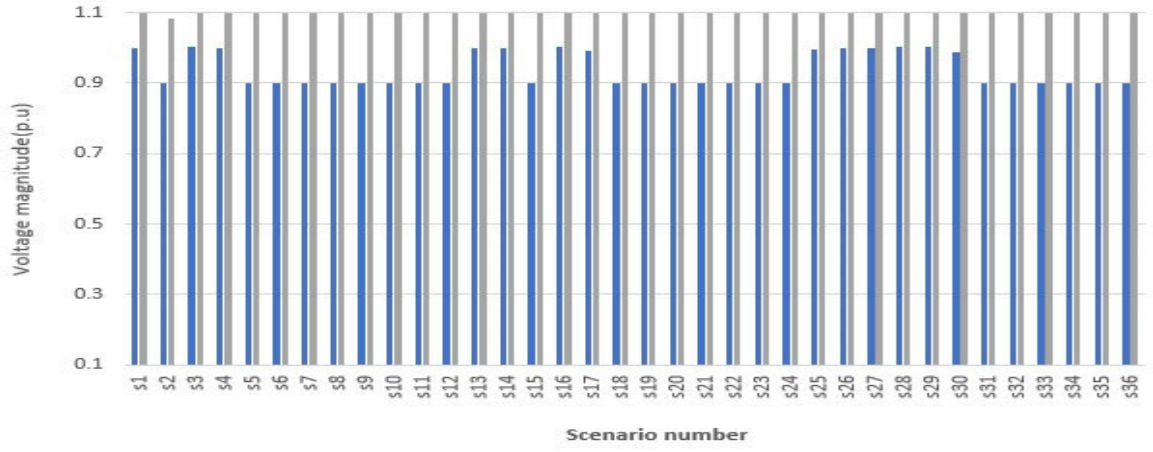

FIGURE 8. Maximum and minimum voltage magnitudes for all scenarios for T1 (Case II).

post-contingency scenarios. The results, which are displayed in Table 8, demonstrate that as the load level is raised, the ATC value for any transaction lowers. It is also obvious that, when compared to the results of the second stage of Case I, the value of ATC at any transaction for the same load level is marginally higher. The most severe contingencies associated with each load level are also exhibited in the table, illustrating how the estimated ATC value was established by accounting for several severe contingencies to enable the system to endure a variety of potentially uncertain conditions. Fig. 8 presents the lowest and highest voltages for each scenario for the second-level problem at 100% of the system's typical load for T1. The diagram shows that the proposed approach can be used to achieve the transaction in all cases while keeping the voltages within the minimum and maximum voltage limits. The expected ATC values in Case II are higher than Case I for

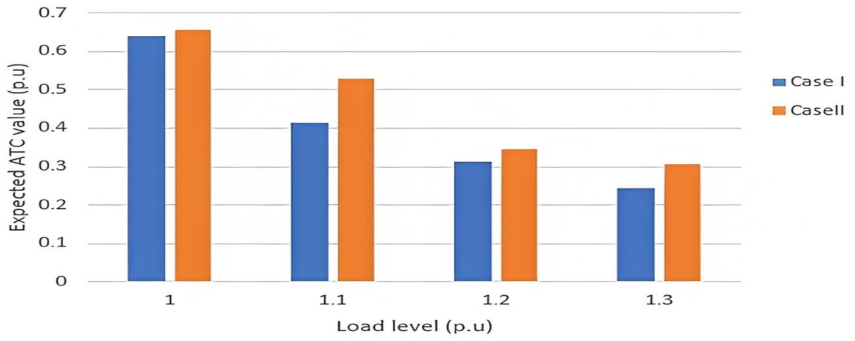

FIGURE 9. Expected ATC values of T1 for the case I and case II.

TABLE 8. Expected ATC value for the second stage (Case II).

Transaction	Load level(p.u)	Expected ATC value (p.u)		Most_severe contingency case for each scenario
		Base _case	Post-contingency case	
T1	1	0.771	0.655	Line1-3 (for s1, s3, s4, s13, s14, s16, s17, s25, s26 s27, s28, s29, s30)
				Line2-6 (for s2 , s15)
				Line22-24 (for s5, s12, s18, s 31)
				Line1-2 (for the other scenarios)
	1.2	0.436	0.347	Line1-2 (for s1, s7, s8, s13, s14, s15, s20, s21, s22, s26, s27, s28, s32, s33, s34, s35, s36)
				Line2-6 (for s6, s19)
				Line 1-3 (for the other scenarios)
	1.3	0.330	0.308	Line1-3 (for s4, s5, s18, s25, s26, s31)
				Line2-6 (for s6, s7, s19, s20, s32, s33)
				Line1-2 (for the other scenarios)
	1.1	0.569	0.529	Line 1-2 (for s3, s4, s5, s16, s17, s18, s29, s30, s31 ,s32)
				Line2-6 (for s1, s2, s13, s14, s15, s27, s28)
				Line22-24 (for s12)
				Line1-3 (for the other scenarios)
T2	1	0.704	0.641	Line 1-3 (for s1, s2, s13, s14, s25, s26, s27)
				Line9-11 (for s3, s4, s5, s6, s15, s16, s17, s18, s19, s28, s29, s30, s31, s32)
				Line22-24(for the other scenarios)
	1.2	0.441	0.406	Line1-2(for s2, s3, s4, s15, s16, s17, s18 , s 28,s29 ,s30, s31, s32)
				Line2-6 (for s1, s13, s14, s27)
				Line 1-3 (for the other scenarios)
	1.3	0.353	0.279	Line1-2 (for s4, s5, s6, s17, s18, s19, s20, s30, s31 s32, s33)
				Line2-6 (for s2, s3, s15, s16, s28, s29)
				Line 1-3(for the other scenarios)
	1.1	0.645	0.565	Line1-2 (for s1, s14, s15, s27, s28)
				Line1-3 (for s2, s 3, s 4, s 5, s16, s17, s18, s25, s26 s29, s 30)
				Line2-6(for s13)
				Line9-11(for s6, s7, s8, s19, s20, s31, s32, s33, s34)
				Line22-24(for the other scenarios)

each transaction, as illustrated in Fig. 9. This is because the wind farm is situated in the sink area of the transaction, which reduces tie line losses and, as a result, increases transmission capacity.

C. CASE III: INCREASING PENETRATION LEVEL OF WIND POWER AT THE GENERATION AREA

In this examination, the penetration level at the generation area is steadily increased under normal system load to

TABLE 9. Settings of VAR devices and expected ATC value for the first stage for T1 (Case III).

Penetration level	Transaction	Optimal setting of VAR resources(p.u)						Expected ATC value for post-contingency case (p.u)
		Qc_{10}	Qc_{24}	T (6-9)	T (6-10)	T (4-12)	T (28-27)	
110%	T1	0.391	0.384	0.900	1.082	0.984	0.972	0.691
120%	T1	0.151	0.078	1.005	1.018	0.966	1.039	0.721
130%	T1	0.031	0.094	1.085	0.955	1.075	1.044	0.737
140%	T1	0.125	0.176	1.023	1.068	1.002	1.054	0.742
150%	T1	0.069	0.354	0.956	1.089	1.075	0.903	0.728
160%	T1	0.061	0.399	0.905	1.088	1.022	0.913	0.719

TABLE 10. Settings of VAR devices and expected ATC value for first stage for T2 (Case III).

Penetration level	Transaction	Optimal setting of VAR resources(p.u)						Expected ATC value for post-contingency case (p.u)
		Qc_{10}	Qc_{24}	T (6-9)	T (6-10)	T (4-12)	T (28-27)	
120%	T2	0.059	0.381	0.931	0.901	0.912	0.992	0.613
140%	T2	0.005	0.329	0.901	0.974	1.085	0.913	0.621
160%	T2	0.398	0.043	1.010	0.959	0.918	1.065	0.626
180%	T2	0.334	0.002	0.939	1.098	0.942	0.936	0.630
200%	T2	0.184	0.215	1.008	0.910	0.910	0.904	0.635
220%	T2	0.004	0.399	1.100	1.098	1.089	0.900	0.641
240%	T2	0.029	0.048	1.002	0.931	1.060	1.023	0.643
260%	T2	0.208	0.032	0.903	1.049	1.099	1.094	0.644
280%	T2	0.363	0.230	1.099	1.027	0.952	0.954	0.643

illustrate how it influences ATC values. With the wind power scenarios utilized in the earlier cases, the first stage is solved. The settings of VAR devices and the anticipated ATC values are listed in Tables 9 and 10, respectively, for T1 and T2. The results show that the predicted ATC values for T1 and T2 are greater than those for the first stage of the preceding cases. Additionally, the results showed that the expected ATC value increases with increasing penetration level up to a point where the TL power losses are raised, at which event the ATC value begins to decline. The rise in TL losses indicates that the TL is being heated up more, which would lead to the TL thermal limit, one of the primary constraints in the ATC evaluation, being reached.

Another crucial aspect is that the increase in the reactive losses can result in inadequate reactive power supply, which will decrease the voltage stability load margin. This indicates that the system is getting close to being unstable and that the penetration level increase needs to be stopped. The maximum penetration is 140% for T1, while for T2 it is 260%, as shown in Table 9 and Table10. The second stage is solved by using the same wind and load scenarios employed in the previous cases for a more accurate ATC evaluation. Table 11 lists the results for T1, which shows the expected ATC value for the base case, the post-contingency case, and the most severe contingency case relevant to each scenario. The results indicated that the predicted ATC value rises with increasing penetration level up to a point of 140%, after which it decreases due to the increased power losses of the transmission lines.

D. CASE IV: ATC EVALUATION WITHOUT VAR DISPATCH

To demonstrate the effect of VAR dispatch of the installed devices on the anticipated ATC value, the simulation is performed for similar prior scenarios with a fixed setting of VAR devices provided in the system data. ATC is evaluated for bilateral and multilateral transactions with the wind power scenarios depicted in Table 2 combined with the load scenarios of each load level shown in Table 3. Table 12 and Table 13 list the results for the case of the location of a wind farm at bus 2 (source area) and bus 28 (sink area), respectively. The results display the expected ATC value for the base and post-contingency cases for each load level, as well as the most severe contingency related to each scenario. As shown in the tables, the expected ATC values are lower with a fixed setting of installed VAR devices when compared to similar cases with VAR dispatch. Also, as observed from the results

TABLE 11. Expected ATC value for the second stage for T1 (Case III).

Penetration level	Transaction	Expected ATC value (p.u)		Most_severe contingency case for each scenario
		Base _case	Post-contingency case	
110%	T1	0.784	0.650	Line1-3 (for s1, s 2, s3, s13, s14, s25, s26, s27)
				Line2-6 (for s15, s28)
				Line 22-24(for the other scenarios)
120%	T1	0.785	0.678	Line 2-6(for s15)
				Line22-24 (for s6, s7, s20, s21, s33, s34, s35, s36)
				Line1-3 (for the other scenarios)
130%	T1	0.789	0.687	Line 2-6 (for s15)
				Line22-24 (for s6, s7, s 8, s11, s 12, s19, s 20, s21, s22, s33, s34, s 35, s36)
				Line1-3 (for the other scenarios)
140%	T1	0.793	0.694	Line2-6 (for s27)
				Line22-24 (s5, s 6, s 7, s11, s12, s15, s19, s20, s21 s33, s34)
				Line1-3 (for the other scenarios)
150%	T1	0.782	0.687	Line2-6 (for s27)
				Line22-24 (s6, s7, s8, s19, s20, s 21, s32, s33,s 34, s35, s36)
				Line1-3 (for the other scenarios)

TABLE 12. Expected ATC value for Case V for wind farm at the source area.

Transaction	Load level(p.u)	Expected ATC value (p.u)		Most severe contingency for each scenario
		Base _case	Post-contingency case	
T1	1	0.477	0.434	Line 1-2(s1, s2, s13, s14, s25, s26, s27)
				Line 1-3(For the other scenarios)
	1.2	0.265	0.148	Line1-2(s3, s4, s16, s17,s28, s29)
				Line2-6(15)
				Line1-3(For the other scenarios)
	1.3	-		
	1.1	0.388	0.335	Line1-2(s1, s2, s3 ,s14, s16, s27, s28)
				Line2-6(s13, s26)
				Line1-3(For the other scenarios)
T2	1	0.383	0.353	Line 1-2(for s25)
				Line 1-3(for the other scenarios)
	1.2	0.248	0.201	Line1-2(s1, s2,s3, s13, s14, s15, s16,s 25,s26,s27, s28)
				Line1-3(For the other scenarios)
	1.3	-		
	1.1	0.318	0.281	Line 1-2(s1,s2 ,s13 ,s14, s25, s26, s27)
				Line 1-3(For the other scenarios)

at 130% of the normal load, the system cannot transfer power except in the case of a multi-lateral transaction with the wind farm at the sink area.

This observation demonstrates VAR dispatch's superiority, as the system can transfer power for any transaction at higher load levels due to more reactive injection. The case of raising the penetration level for T1 as simulated in Case III has also been explored here when fixing VAR devices. The outcomes for the same prior instance of increasing penetration level for T1 with a fixed setting of VAR devices are shown in

TABLE 13. Expected ATC value for Case IV for wind farm at the sink area.

Transaction	Load level(p.u)	Expected ATC value (p.u)		Most severe contingency for each scenario
		Base _case	Post-contingency case	
T1	1	0.543	0.519	Line 1-2(For all scenarios)
	1.2	0.334	0.237	Line1-3(s1, s2, s13, s14 , s15, s25, s26, s27, s28)
				Line2-6(s3, s16, s29)
				Line 1-2(For the other scenarios)
	1.3	-		
	1.1	0.462	0.431	Line1-3(s25)
				Line2-6(s13, s26)
				Line1-2(For the other scenarios)
T2	1	0.438	0.417	Line1-2(s5, s 6, s18, s19, s25, s26 s31 s32)
				Line 1-3(For the other scenarios)
	1.2	0.314	0.278	Line1-3(s10, s23, s24)
				Line 1-2(For the other scenarios)
	1.3	0.209	0.128	Line1-3(s1, s13, s14, s25, s26, s27)
				Line2-6(s15, s28)
				Line 1-2(For the other scenarios)
	1.1	0.380	0.353	Line1-3(s5, s6, s7, s11, s12, s18,s19, s20, s32, s33)
				Line 1-2(For the other scenarios)

TABLE 14. Expected ATC value for Case IV with increasing penetration level.

Penetration level	Transaction	Expected ATC value (p.u)		Most_severe contingency case for each scenario For fixed dispatch
		Base _case	Post-contingency case	
110%	T1	0.480	0.439	Line1-2(s1,s2 ,s13,s14, s25,s26)
				Line1-3(for the other scenarios)
120%	T1	0.484	0.444	Line1-2(s1,s2 ,s13,s14, s25,s26)
				Line1-3(for the other scenarios)
130%	T1	0.487	0.449	Line1-2(s1,s2 ,s13,s14, s25,s26)
				Line1-3(for the other scenarios)
140%	T1	0.491	0.454	Line1-2(s1,s2 ,s13,s14, s25,s26)
				Line1-3(for the other scenarios)
150%	T1	0.494	0.459	Line1-2(s1,s2 ,s13,s14, s25,s26)
				Line1-3(for the other scenarios)

Table 14. As compared to the identical scenario with VAR dispatch of installed devices, the results show that expected ATC values were reduced. The results of this case show that the most severe lines for most load levels for any transaction are less than they were in the previous cases (VAR dispatch cases). This indicates that the dispatch of installed devices allows the system to be more secure by withstanding more significant outages that might unintentionally occur. The above results emphasize the significance of effectively utilizing the installed VAR sources regulated by the TSO to improve power transfer between zones as well as increase system security.

Finally, the contributions of this work have been validated in the simulation results as follows:

- The achieved results of the second stage in the previous cases ensure a more precise ATC evaluation close to real time by including more scenarios of the load and wind power into the problem formulation. As a result, projected ATC values are provided with more precision, giving renewable energy participants the chance to trade

with less risk and enhancing the efficiency of market transactions.

- The acquired results for case V when compared to other cases demonstrate the critical role that installed VAR devices play in maximizing ATC values for various transactions at various wind farm locations.
- The first-stage results for the prior cases have shown that the proposed hybrid IGWO/PDIPM solution approach has been able to determine the common adequate setting for installed VAR devices for all investigated hourly scenarios. These settings are employed as a preventive control in the second stage, where they are held constant for a predetermined period of time to reduce unwanted status changes and excessive operation of VAR devices.

VII. CONCLUSION

This paper introduces a method for evaluating available transfer capacity in an intraday market while considering the concerns of voltage stability as well as the uncertainties of the anticipated load and wind power. The presented approach seeks to maximize expected ATC value and increase transaction between various zones by enhancing the usage of the existing VAR sources. A two-stage framework has been proposed to achieve this purpose, with the first stage concentrating on the selection of appropriate VAR settings that improve the ATC value a few hours before the real state, and the second stage focusing on the ATC assessment near the delivery time to enhance the accuracy of the ultimate ATC value. The proposed methodology enables the transmission system operator to assess ATC near the actual state, allowing wind energy participants to increase their level of integration without putting them at severe risk. The problem is solved using a two-level hybrid approach that combines the improved grey wolf optimizer with the primal-dual interior point method. The proposed approach is implemented on the IEEE 30-RTS. The outcomes show the applicability of the proposed technique to evaluate and maximize ATC value for bilateral and multilateral transactions while considering the placement of wind farms at the source area and sink area. The results indicated that wind farms had a greater beneficial impact on ATC value when installed close to the sink area than when installed at the source area. Additionally, it is indicated that the proposed method could identify the most severe contingency related to each scenario, which is crucial for the system operator to take into account when planning for any transaction to withstand a number of unexpected circumstances. The investigation of the impact of wind power penetration on the predicted ATC value has shown that the level of penetration is an important factor that should be precisely assessed to positively affect the ATC value; otherwise, its effect may be adverse. The results also emphasize the significance of carrying out optimal VAR dispatch of installed VAR devices owned by TSO along with dispatch of generated active power in the ATC estimate in order to achieve more efficient power transfer across zones and improve system security. Even though the viability of the problem and the validity of the formulation have been demonstrated in this work, additional issues are required to be incorporated into the presented formulation in order to make it more comprehensive. The expansion of the current formulation to take into account the TRM and CBM, the variability of wind power and load, as well as the reactive power capability of the DFIG are the concerns that are now being investigated. The formulation can also be easily expanded to explore the optimal placement of new FACTS devices, which primarily influence the ATC value for the anticipated stressed network due to the increase in network load. Such research is essential for the Egyptian system, which has recently undergone a significant integration of renewable energy sources in locations beyond the load center.

REFERENCES

[1] S. D. Ahmed, F. S. M. Al-Ismail, M. Shafiullah, F. A. Al-Sulaiman, and I. M. El-Amin, "Grid integration challenges of wind energy: A review," *IEEE Access*, vol. 8, pp. 10857–10878, 2020, doi: 10.1109/ACCESS.2020.2964896.

[2] *Available Transfer Capability Definitions and Determination*, North Amer. Electr. Realiability Corp., 1996, pp. 1–42. Accessed: Apr. 19, 2023. [Online]. Available: http://www.ece.iit.edu/~flueck/ece562/atcfinal.pdf

[3] L. Min and A. Abur, "Total transfer capability computation for multi-area power systems," *IEEE Trans. Power Syst.*, vol. 21, no. 3, pp. 1141–1147, Aug. 2006, doi: 10.1109/TPWRS.2006.876690.

[4] Z. Chen, M. Zhou, and G. Li, "ATC determination for the AC/DC transmission systems using modified CPF method," in *Proc. 5th Int. Conf. Crit. Infrastructure (CRIS)*, Sep. 2010, pp. 1–8, doi: 10.1109/CRIS.2010.5617512.

[5] J. Liu, Y. Liu, G. Qiu, and X. Shao, "Learning-aided optimal power flow based fast total transfer capability calculation," *Energies*, vol. 15, no. 4, p. 1320, Feb. 2022, doi: 10.3390/en15041320.

[6] X. Fang, F. Li, N. Gao, and Q. Guo, "Available transfer capability of photovoltaic generation incorporated system," in *Proc. IEEE PES Gen. Meeting Conf. Expo.*, Jul. 2014, pp. 1–5, doi: 10.1109/PESGM.2014.6939938.

[7] X. Pan and G. Xu, "Available transfer capability calculation considering voltage stability margin," *Electric Power Syst. Res.*, vol. 76, nos. 1–3, pp. 52–57, Sep. 2005, doi: 10.1016/j.epsr.2005.04.006.

[8] G. Hamoud, "Assessment of available transfer capability of transmission systems," *IEEE Trans. Power Syst.*, vol. 15, no. 1, pp. 27–32, Feb. 2000, doi: 10.1109/59.852097.

[9] A. K. Sharma and J. Kumar, "ACPTDF for multi-transactions and ATC determination in deregulated markets," *Int. J. Electr. Comput. Eng. (IJECE)*, vol. 1, no. 1, pp. 71–84, Sep. 2011, doi: 10.11591/ijece.v1i1.61.

[10] P. Kerur and R. L. Chakrasali, "Power transfer capability recognition in deregulated system under line outage condition using power world simulator," *J. Electr. Eng. Autom.*, vol. 3, no. 4, pp. 277–285, Jan. 2022, doi: 10.36548/jeea.2021.4.003.

[11] A. B. Rodrigues and M. G. Da Silva, "Probabilistic assessment of available transfer capability based on Monte Carlo method with sequential simulation," *IEEE Trans. Power Syst.*, vol. 22, no. 1, pp. 484–492, Feb. 2007, doi: 10.1109/TPWRS.2006.887958.

[12] M. M. B. Othman, A. Mohamed, and A. Hussain, "Determination of transmission reliability margin using parametric bootstrap technique," *IEEE Trans. Power Syst.*, vol. 23, no. 4, pp. 1689–1700, Nov. 2008, doi: 10.1109/TPWRS.2008.2004734.

[13] O. O. Mohammed, M. W. Mustafa, D. S. S. Mohammed, and A. O. Otuoze, "Available transfer capability calculation methods: A comprehensive review," *Int. Trans. Electr. Energy Syst.*, vol. 29, no. 6, pp. 1–24, Jun. 2019, doi: 10.1002/2050-7038.2846.

[14] X. Kou, S. Member, and F. Li, "Interval optimization for available transfer capability evaluation considering wind power uncertainty," *IEEE Trans. Sustain. Energy*, vol. 11, no. 1, pp. 250–259, Jan. 2020, doi: 10.1109/TSTE.2018.2890125.

[15] A. M. Alshamrani, M. A. El-Meligy, M. Sharaf, W. A. M. Saif, and E. M. Awwad, "Transmission expansion planning considering a high share of wind power to maximize available transfer capability," *IEEE Access*, vol. 11, pp. 23136–23145, 2023, doi: 10.1109/ACCESS.2023.3253201.

[16] X. Sun, Z. Tian, Y. Rao, Z. Li, and P. Tricoli, "Probabilistic available transfer capability assessment in power systems with wind power integration," *IET Renew. Power Gener.*, vol. 14, no. 11, pp. 1912–1920, Aug. 2020, doi: 10.1049/iet-rpg.2019.1383.

[17] A. Narain, S. K. Srivastava, and S. N. Singh, "Impact of wind power generation on ATC calculation with uncertain equal load," *Electr. Eng.*, vol. 104, no. 1, pp. 3–11, Feb. 2022, doi: 10.1007/s00202-020-01159-4.

[18] O. O. Mohammed, M. W. Mustafa, S. Salisu, A. Memon, S. Hussain, A. O. Otuoze, and O. Ibrahim, "Assessment of the influence of wind energy incorporated capacity benefit margin in ATC computation," *Int. J. Appl. Power Eng. (IJAPE)*, vol. 11, no. 2, p. 145, Jun. 2022, doi: 10.11591/ijape.v11.i2.pp145-155.

[19] H. Chen, X. Fang, R. Zhang, T. Jiang, G. Li, and F. Li, "Available transfer capability evaluation in a deregulated electricity market considering correlated wind power," *IET Gener., Transmiss. Distrib.*, vol. 12, no. 1, pp. 53–61, Jan. 2018, doi: 10.1049/iet-gtd.2016.1883.

[20] D. Chen, Z. Chen, H. Fan, X. Xu, M. Liu, and Y. Chen, "Probability evaluation method of available transfer capability considering source-load side uncertainty," in *Proc. 4th Int. Conf. Power Energy Technol. (ICPET)*, Jul. 2022, pp. 47–52, doi: 10.1109/ICPET55165.2022.9918213.

[21] T. Jiang, X. Li, X. Kou, R. Zhang, G. Tian, and F. Li, "Available transfer capability evaluation in electricity-dominated integrated hybrid energy systems with uncertain wind power: An interval optimization solution," *Appl. Energy*, vol. 314, May 2022, Art. no. 119001, doi: 10.1016/J.APENERGY.2022.119001.

[22] N. F. Avila and C.-C. Chu, "Distributed probabilistic ATC assessment by optimality conditions decomposition and LHS considering intermittent wind power generation," *IEEE Trans. Sustain. Energy*, vol. 10, no. 1, pp. 375–385, Jan. 2019, doi: 10.1109/TSTE.2018.2796102.

[23] Z. Jinlong, Z. Huilin, B. Yanhong, D. Fangwei, Y. Yingxuan, and Z. Haotian, "On-line assessment method of available transfer capability considering uncertainty of renewable energy power generation," in *Proc. Asia Energy Electr. Eng. Symp. (AEEES)*, Chengdu, China, May 2020, pp. 43–48, doi: 10.1109/AEEES48850.2020.9121466.

[24] A. Narain, S. K. Srivastava, and S. N. Singh, "A novel sensitive based approach to ATC enhancement in wind power integrated transmission system," *Social Netw. Appl. Sci.*, vol. 3, no. 5, pp. 1–10, May 2021, doi: 10.1007/s42452-021-04559-8.

[25] S. K. Alamanda and K. K. Boddeti, "Relative distance measure arithmetic-based available transfer capability calculation with uncertainty in wind power generation," *Int. Trans. Electr. Energy Syst.*, vol. 31, no. 11, pp. 1–17, Nov. 2021, doi: 10.1002/2050-7038.13112.

[26] M. Karuppasamypandiyan, P. A. Jeyanthy, D. Devaraj, and V. A. I. Selvi, "Day ahead dynamic available transfer capability evaluation incorporating probabilistic transmission capacity margins in presence of wind generators," *Int. Trans. Electr. Energy Syst.*, vol. 31, no. 1, pp. 1–21, Jan. 2021, doi: 10.1002/2050-7038.12693.

[27] M. Khosravifard and M. Shaaban, "Risk-based available transfer capability assessment including nondispatchable wind generation," *Int. Trans. Elect. Energy Systems*, vol. 25, no. 11, pp. 3169–3183, 2014, doi: 10.1002/etep.2036.

[28] L. Zhang, Y. Liu, and J. Wang, "Evaluation on available transfer capability of power system considering wind speeds correlation," *J. Softw. Eng.*, vol. 9, pp. 749–760, Jan. 2015, doi: 10.3923/jse.2015.749.760.

[29] Z. C. Li, B. H. Zhang, Y. B. Ge, Y. Chen, X. G. Miao, L. D. Zhang, J. L. Wu, and P. Bie, "Probabilistic available transfer capability calculation of wind farm incorporated power system," *Adv. Mater. Res.*, vols. 724–725, pp. 582–586, Aug. 2013, doi: 10.4028/www.scientific.net/AMR.724-725.582.

[30] *Basics of the Power Market | EPEX SPOT*. Accessed: Apr. 1, 2023. [Online]. Available: https://www.epexspot.com/en/basicspowermarket

[31] S. M. Mohseni-Bonab and A. Rabiee, "Optimal reactive power dispatch: A review, and a new stochastic voltage stability constrained multi-objective model at the presence of uncertain wind power generation," *IET Gener., Transmiss. Distrib.*, vol. 11, no. 4, pp. 815–829, Mar. 2017, doi: 10.1049/iet-gtd.2016.1545.

[32] Y. M. Atwa and E. F. El-Saadany, "Probabilistic approach for optimal allocation of wind-based distributed generation in distribution systems," *IET Renew. Power Gener.*, vol. 5, no. 1, pp. 79–88, 2011, doi: 10.1049/iet-rpg.2009.0011.

[33] A. Dukpa, B. Venkatesh, and L. Chang, "Fuzzy stochastic programming method: Capacitor planning in distribution systems with wind generators," *IEEE Trans. Power Syst.*, vol. 26, no. 4, pp. 1971–1979, Nov. 2011, doi: 10.1109/TPWRS.2010.2103576.

[34] N. Yorino, H. Li, S. Harada, A. Ohta, and H. Sasaki, "A fast estimation of load power margins for generator outage contingencies," *IEEJ Trans. Power Energy*, vol. 122, no. 12, pp. 1348–1354, 2002, doi: 10.1541/ieejpes1990.122.12_1348.

[35] N. Yorino, H. Q. Li, S. Harada, A. Ohta, and H. Sasaki, "A method of voltage stability evaluation for branch and generator outage contingencies," *IEEE Trans. Power Syst.*, vol. 19, no. 1, pp. 252–259, Feb. 2004, doi: 10.1109/TPWRS.2003.818740.

[36] M. H. Nadimi-Shahraki, S. Taghian, and S. Mirjalili, "An improved grey wolf optimizer for solving engineering problems," *Exp. Syst. Appl.*, vol. 166, Mar. 2021, Art. no. 113917, doi: 10.1016/J.ESWA.2020.113917.

[37] S. Mirjalili, S. M. Mirjalili, and A. Lewis, "Grey wolf optimizer," *Adv. Eng. Softw.*, vol. 69, pp. 46–61, Mar. 2014, doi: 10.1016/j.advengsoft.2013.12.007.

HALA W. REYAD received the B.S. degree in electrical power and machines from Port Said University, Egypt, in 2017, where she is currently pursuing the M.S. degree in power system operation with renewable energy in electrical engineering. Since 2018, she has been a Demonstrator with the Department of Electrical Engineering, Faculty of Engineering, Port Said University. Her current research interests include power system analysis, renewable energy sources, and heuristic techniques in power systems.

MEDHAT ELFAR received the Ph.D. degree in electrical engineering from Port Said University, in 2010. Since 2010, he has been an Assistant Professor with the Department of Electrical Engineering, Faculty of Engineering, Port Said University. From June 2014 to December 2014, he was a Postdoctoral Researcher with the Energy Research Center, UOIT University, Canada. He is currently an Assistant Professor with the Department of Electrical Engineering, Faculty of Engineering, Port Said University. His current research interests include power electronics and artificial intelligence applications on electrical machines and renewable energy systems.

E. E. EL-ARABY (Member, IEEE) received the B.S. and M.S. degrees from Suez Canal University, Egypt, in 1990 and 1996, respectively, and the Ph.D. degree from the Department of Artificial Complex Engineering, Hiroshima University, Japan, in 2003. He was a Postdoctoral Fellow with the Department of Artificial Complex Engineering, Hiroshima University, from 2004 to 2006. He was an Associate Professor with Qassim University, Saudi Arabia, from 2007 to 2016. He is currently an Associate Professor with the Department of Electrical Engineering, Port Said University, Port Said, Egypt. His research interests include power system planning, operation, renewable energy integration, and ancillary services pricing in electricity markets.